Annals of Biomedical Engineering, Vol. 46, No. 2, February 2018 (© 2017) pp. 211–221
https://doi.org/10.1007/s10439-017-1962-x

Finite Element Design Optimization of a Hyaluronic Acid-Based Hydrogel Drug Delivery Device for Improved Retention

JOURDAN COLTER,[1] BARBARA WIROSTKO,[2,3] and BRITTANY COATS[1]

[1]Department of Mechanical Engineering, University of Utah, Mechanical Engineering Kennecott Building, 1495 E 100 South, Rm. 1550, Salt Lake City, UT 84112, USA; [2]Jade Therapeutics Inc. (A wholly owned subsidiary of EyeGate Pharmaceuticals Inc.), EyeGate Pharma, 391 Chipeta Way, Suite H, Salt Lake City, UT 84108, USA; and [3]Department of Ophthalmology, Moran Eye Center, University of Utah, 65 Mario Capecchi Dr., Salt Lake City, UT 84132, USA

(*Received 18 July 2017; accepted 13 November 2017; published online 17 November 2017*)

Associate Editor Joel D. Stitzel oversaw the review of this article.

Abstract—Drug-loaded hydrogel devices are emerging as an effective means of localized and sustained drug delivery for the treatment of corneal conditions and injuries. One such device uses a novel, thiolated crosslinked carboxymethylated, hyaluronic acid-based hydrogel (CMHA-S) film to deliver drug to the ocular surface upon placement into the inferior fornix of the eye. While proven to be very safe and effective, the CMHA-S film tends to dislodge in the highly-lubricated ocular environment, thereby reducing drug delivery efficiency and drug efficacy. In this study, we used a three-dimensional computational finite element model of the eye to determine the effect of geometry and surface friction on film retention in the inferior fornix, and to evaluate multiple geometrical film designs. Retention of the film was dependent on geometry and on the friction ratio of the film to the eyelid and globe. These effects were interactive. When the ratio of friction on the lid side to the globe side of the film was low, geometry played a large role in the film's displacement. When this ratio was high, differences in displacement due to geometry were negligible. The optimal relationship of friction between the film and its eyelid-side and globe-side surfaces was found to be linear with at least 1.4 times greater friction required on the eyelid-side for immobilization. A geometry similar to a half cylinder was found to be most effective with this friction ratio in retaining the film in the inferior fornix and in contact with the globe. Other geometries will likely require other friction ratios. In summary, CMHA-S film retention can be achieved through simple modifications of geometry and manipulation of surface interaction with the eye.

Keywords—Ocular drug delivery, CMHA-S, Antibiotics, Ophthalmology, Computation.

Address correspondence to Brittany Coats, Department of Mechanical Engineering, University of Utah, Mechanical Engineering Kennecott Building, 1495 E 100 South, Rm. 1550, Salt Lake City, UT 84112, USA. Electronic mail: brittany.coats@utah.edu

INTRODUCTION

There are a suspected 60 million global cases of glaucoma,[17] and 20 million US cases of chronic dry eye syndrome,[15] which commonly employ liquid eye drops for treatment. If not treated thoroughly and with ongoing care, both can drastically diminish visual quality of life, and even cause blindness in cases of glaucoma.[16] The standard of care treatment using liquid topical drops suffer from several limitations. Self-administration by the patient is often inadequate or inefficient, and results in drop wastage and bottle contamination.[10] Patient compliance is poor, especially in pediatric patients, the elderly, and in drugs prescribed to be administered every 1–3 h.[9,20] In addition to these user error inefficiencies, drug bioavailability is often less than 5% due to quick drug removal by the tear production, the drainage system and competition with other non-intended tissues.[21] All these inefficiencies of topical eye drops can lead to reduced healing, less than optimal visual outcomes, and even drug-resistance development when treating these pathologic ophthalmic conditions.

Drug-loaded, hydrogel polymers are emerging as an effective means of localized and sustained drug delivery for treatment of ophthalmic conditions. Hydrogels can be easily manipulated to control for shape, degradation, drug-release, and biomechanical properties to enhance and customize therapeutic effects for specific ophthalmic applications. For example, careful control of degradation rates through cross-linking can create hydrogels that last for weeks or months, yielding an ophthalmic product that can offer a controlled and slow-releasing drug delivery that has more efficient uptake by the targeted ocular tissues.

Jade Therapeutics Inc. (wholly owned subsidiary of EyeGate Pharmaceutical, Inc., Salt Lake City, UT, USA) has developed a polymer film that is able to release drug to the ocular surface using a localized and controlled delivery method. Their polymer is based on a novel and proprietary, thiolated crosslinked carboxymethylated, hyaluronic acid-based, hydrogel (CMHA-S). The CMHA-S film is soft, pliable, and transparent when hydrated, and has proven to be safe and tolerable in the eye.[8,18,25,26] A gelled version of CMHA-S is presently sold commercially as a veterinary liquid eye drop, as Remend® Corneal Repair (SentrX Animal Care, Salt Lake City, UT, USA), and sold globally by Bayer Animal Health. This product is indicated for use in the management of superficial corneal ulcers,[24] and has been used for 5 years in dogs, cats and horses, with an excellent safety record. Hyaluronic acid (HA), a naturally occurring polysaccharide in the body, provides additional medicinal benefit to the CMHA-S film by contributing to lubrication and tissue repair.[22] HA-based topical eye drops are the standard of care around the world, and being used as lubricating eye drops in humans. Crosslinking HA to get CMHA-S allows for hydrogels to be tailored in the form of thin films, sponges or gels. While the lubricating quality of HA increases comfort and tolerability of the hydrogel film in the eye, it coats the film surface and results in poor ocular retention. A recent pilot *in vivo* rabbit study from our group documented that CMHA-S films tended to migrate out of the inferior fornix after a couple days, which eventually resulted in complete dislodging from the inferior fornix. Careful control of the interaction and retention of the hydrogel films with the eye is needed to achieve a longer duration of drug administration.

One potential way to improve retention is through geometrical alteration. In early design prototyping of these hydrogels, it was observed that rolled films were generally retained better than flat films. It was unclear why this was the case, and resulted in the need for a more thorough evaluation of geometric features which would lead to better retention. One way to glean this information is through computational finite element (FE) analysis. Designing a FE model that is representative of the hydrogel in the inferior fornix of the eye would be useful in understanding the geometrical and mechanical contributions to film displacement. Additionally, the FE model would be able to quickly test the viability of various design alterations, in comparison to spending additional time and resources molding and testing various designs *in vivo*.

While geometrical optimization may lead to improved retention, control of frictional interactions of the hydrogel with the eye will likely play a critical role. The friction of the CMHA-S film with the eye is currently unknown. However, similar hydrogel materials yield coefficients of friction with low orders of magnitude. Roba *et al*. quantified the coefficient of friction of high-water, hydrogel contact lenses to be as low as 0.02 and as high as 0.5.[19] A similar range of coefficient of friction values was found for polyacrylic acid hydrogels (0.05–0.3),[12] while a slightly higher range was reported for varied formulations of polyvinyl alcohol hydrogels (0.3–0.9).[3] This relatively large range in coefficients of friction reported in the literature is due to wide differences in material stiffness, opposing sliding surface, and lubrication methods. Despite this variability, the frictional properties of hydrogel materials highly improve the functionality of ocular, artificial joint, and surface-coating applications; and the coefficient of friction values are tightly controlled to achieve the optimal function in each application. Given this sensitive nature of a hydrogel's functionality due to its coefficient of friction, it is hypothesized that altering the frictional interactions of the CMHA-S hydrogel with the eye will highly impact the hydrogel film's displacement in the eye. Therefore, optimizing the relationship of the coefficients of friction of the hydrogel and globe to the hydrogel and lower eyelid for improved retention will be important in reducing displacement.

The goal of this study was to build a human eye FE model to (1) identify a potential film geometry for better retention in the inferior fornix, and to (2) determine an ideal friction relationship of the hydrogel with the globe and eyelid for hydrogel film immobilization. To achieve this, parametric simulations were run that varied a hydrogel film through eight designs, and iteratively ran through a range of coefficient of friction values on each side of one hydrogel geometry to test the retention due to many coefficient of friction pairs. Outcomes from the model will inform the final design of the EyeGate/Jade Therapeutics' CMHA-S drug delivery device.

METHODS

Model Geometry

A finite element model was developed that consisted of a globe, lower eyelid, and hydrogel film (Fig. 1). The globe was simplified as a spherical shell with a diameter of 22 mm, which is similar to that of an adult, human eye.[4] A 0.25 mm thick lower eyelid, was placed in direct surface-to-surface contact with the inferior portion of the globe. The hydrogel film was placed between the globe and eyelid in a manner that allowed realistic compression of the hydrogel against the globe. Meth-

ods to achieve this are discussed in detail in Section "Boundary Conditions and Contact Interactions."

Initial prototypes developed by Jade Therapeutics were molded as flat, rectangular films. Observations noted that these flat films were inclined to roll up on themselves after rehydration. Early evaluation suggested that these rolled films tended to have better retention than the flat films. Therefore, eight different hydrogel film geometries were designed and analyzed in the model, representing various iterations of this preferred cylindrical shape (Fig. 2). All geometries were designed to be the final swelled shape that would be achieved after film hydration. The half-life of these films is greater than 1 week, so degradation was not considered. Geometry 1 was a solid and perfect cylinder replicating the rolled flat film of 3 mm diameter. Geometries 2 and 3 were half-cylindrical in shape, with Geometry 2 having a flat surface in contact with the globe, and Geometry 3 having a slightly-rounded surface. Geometry 4 was designed as the smaller version of Geometry 1, because Geometry 1 was very large in relation to the globe. Out of these first 4 geometries, preliminary simulations deemed that Geometry 2 performed the best. Thus, Geometry 5 was designed similar to Geometry 2, but with its flat side against the eyelid. It was hypothesized that Geometry 5 would have better retention, since it had more contact with the eyelid. Geometries 6–8 were designed as the less-bulky and flatter versions of Geometry 5 by reducing two or more dimensions of thickness, width, or length. The dimensions were designed to generate a volume of 30 μL based on desired drug loading concentrations and release profiles. All geometry dimensions, including thickness, length, width and volume, are listed in Fig. 2.

Material Properties

The hydrogel film was modeled as a hyper- and viscoelastic solid. Hydrogel material data were obtained in lab using uniaxial tensile testing with sterilized and rehydrated films of the desired formulation (CMHA-S, Jade Therapeutics Inc., SLC). Specimens were subjected to both stress-relaxation and pull-to-failure tests while submerged in a phosphate-buffered saline solution.[5] A number of hyperelastic material models were considered using the ABAQUS Material Evaluator (v6.12-2, Dassault Systemes Simulia Corp., Vlizy-Villacoublay Cedex, France).

Common constitutive models, such as the Mooney-Rivlin and second-order Ogden models, provided good fits to the data, but were considered unstable by ABAQUS (Fig. 3a). Therefore, a Marlow hyperelastic model was selected because it was able to replicate the uniaxial test data exactly, and reasonably estimates other modes of deformation for isotropic and nearly incompressible materials.[13] The equation of the Marlow model strain energy potential is

$$U = U_{\text{dev}}(\bar{I}_1) + U_{\text{vol}}(J_{\text{el}}) \tag{1}$$

where U is the strain energy per unit of reference volume, with U_{dev} and U_{vol} as its deviatoric and volumetric parts, respectively; and J_{el} is the elastic volume ratio. The first deviatoric strain invariant, $\bar{I}_1$, is defined by

$$\bar{I}_1 = \bar{\lambda}_1^2 + \bar{\lambda}_2^2 + \bar{\lambda}_3^2 \tag{2}$$

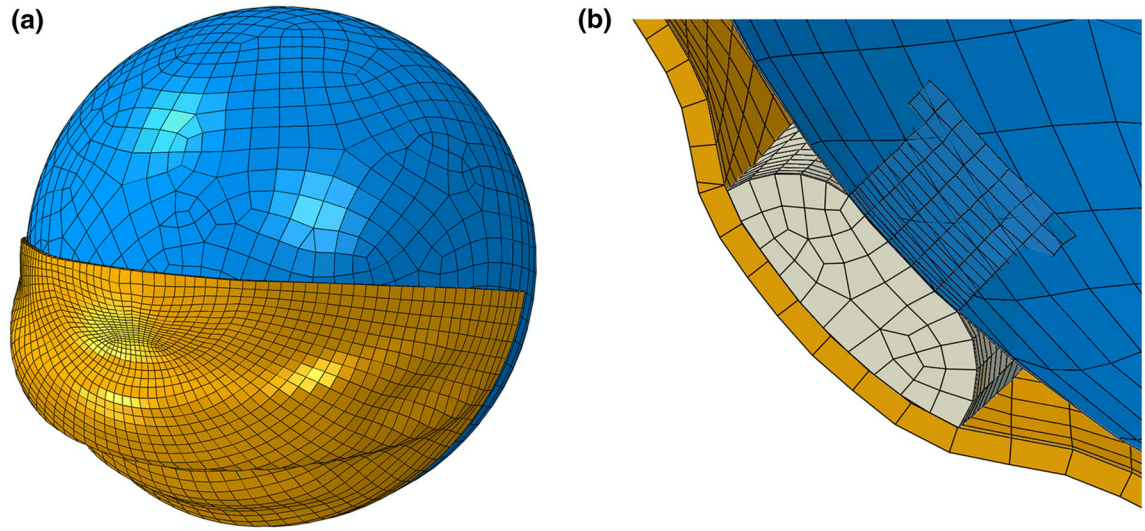

FIGURE 1. (a) Simplified globe, lower eyelid, and hydrogel film representing film placement in the inferior fornix. (b) Cross-section of the film placed between the globe and lower eyelid.

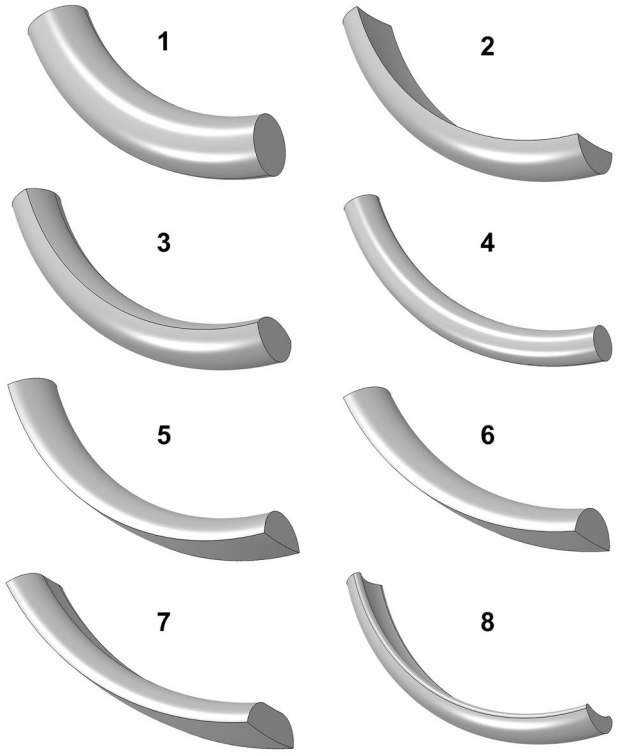

Geometry	1	2	3	4	5	6	7	8
Thickness (mm)	3	1.5	2	1.5	1.5	1.25	1	0.88
Length (mm)	15	15	15	15	15	12.2	11.7	17.6
Width (mm)	3	3	3	1.5	3	2.5	3	2.5
Volume (μL)	106	47	73	26	55	30	30	30

FIGURE 2. SolidWorks renderings and dimensions of the eight hydrogel film geometries that were designed and simulated in the model. Geometries are not shown to scale.

where the deviatoric stretches are

$$\bar{\lambda}_i = J^{-1/3}\lambda_i \tag{3}$$

where J is the total volume ratio, and λ_i are the principal stretches. In this case, the deviatoric part of the potential is defined by uniaxial test data, and the volumetric part is defined by the Poisson's ratio.

Hydrogel film viscoelastic stress-relaxation data was fit with a Prony-series approximation (Fig. 3b). The density and Poisson's ratio were selected to be similar to water, because hydrogels have very high water content ($> 90\%$).[2,7] Due to computational limitations modeling a purely incompressible material such as water, Poisson's ratio was chosen to represent a nearly incompressible material with a value of 0.49. A hyperelastic and viscoelastic model was selected over a poroelastic model because preliminary evaluations indicated small compressions during placement of the film in the eye and no additional compression during globe rotation. This suggested a poroelastic model

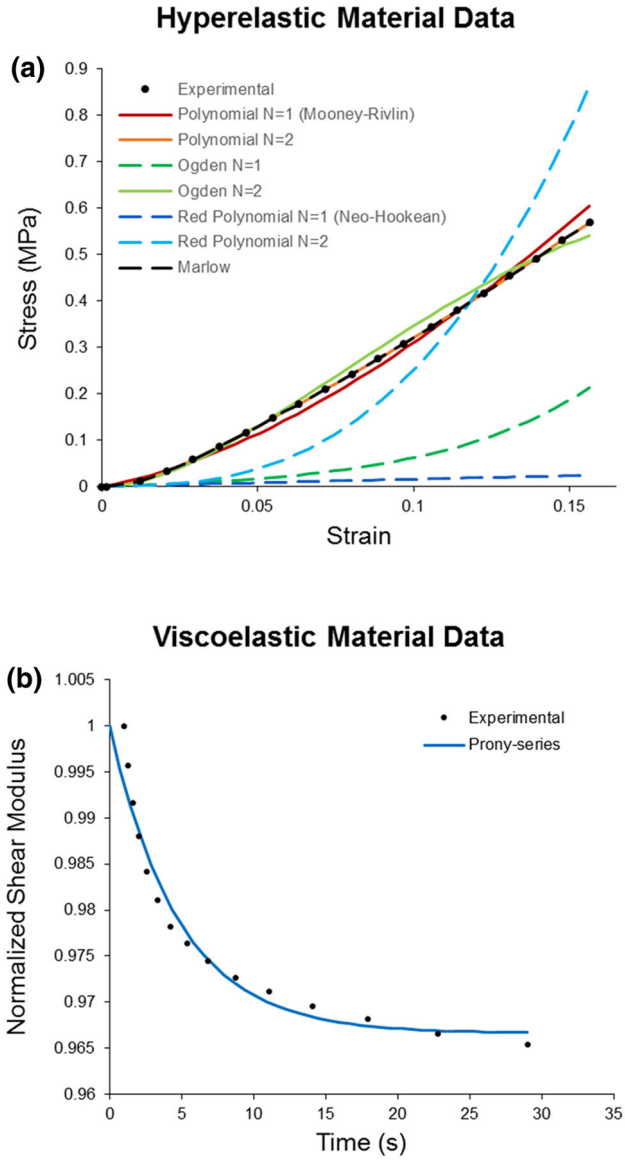

FIGURE 3. (a) Hyperelastic experimental data and material fits from ABAQUS Material Evaluator. Dashed lines indicate constitutive models that are stable, while solid lines indicate those that are unstable. (b) Viscoelastic experimental data and Prony-series approximation.

would not likely influence displacement of the hydrogel during globe rotation.

The lower eyelid was modeled as an isotropic, linear-elastic solid with the properties of skin. Specifically, the elastic modulus was defined as 58.2 MPa, which is found to be in the range of elasticities reported for adult skin in the literature.[1,6] Values of 0.49 and g/cm^3 were assigned for the Poisson's ratio and density of skin, respectively.[11,14]

Due to intraocular pressure and the stiff mechanical properties of sclera compared to the hydrogel, the globe was assumed to experience minimal deformation

during placement of the hydrogel and eye rotation. To verify this assumption, measured hyper- and viscoelastic properties of sclera were incorporated into the model. Maximum principal strain was 2×10^{-7}, suggesting approximating the globe as rigid body is an adequate assumption and greatly reduces computational time. A list of all material parameters used in the inferior fornix model can be found in Table 1.

Mesh

All geometry meshing was performed in ABAQUS. The globe was meshed with hybrid, linear quadrilateral and triangular shell elements. The lower eyelid and all eight hydrogel film geometries were meshed with linear hexahedral elements. A mesh convergence study was run, and found nodal displacements to converge. A mesh density was selected, in which the average nodal displacement of the hydrogel film was within 27% error from the finest mesh density evaluated. Mesh densities for the globe and lower eyelid components were defined by global seed sizes of 0.001 and 0.0005, respectively. In order to maintain constant mesh density across the films, a global seed size of 0.0003 was used for all film design iterations.

The number of nodes, number of elements, and mesh quality for each model component can be found in supplementary material Table S1. Mesh quality was determined by extracting average elemental aspect ratios for each model component. Aspect ratios under 2.5 were deemed good for this analysis. The lower eyelid had some elements above this threshold (worst = 4.13), but these elements were in the periphery, not in highly deforming areas, and would not affect hydrogel displacement.

Boundary Conditions and Contact Interactions

The simulation was executed in two steps: a hydrogel film placement step, and a globe rotation step. In the placement step, the hydrogel film originated inside the globe with the eyelid lying flat and in direct contact with the globe. The posterior edge of the eyelid was fixed in translational degrees of freedom, and the globe was fixed in all degrees of freedom so that it was immobilized. Contact between the globe and the hydrogel was muted to allow the hydrogel to pass through the globe during placement. Specifically, the hydrogel was displaced out of the globe by 2–4 mm (depending on the geometry), which pushed the eyelid away from the globe until the hydrogel inner surface was in contact with the outer surface of the globe. This allowed the eyelid to deform around the hydrogel shape, which physiologically replicated the lower eyelid being deformed during hydrogel placement in the inferior fornix.

During the globe rotation step, displacement of the hydrogel was terminated and contact was established between the hydrogel and globe. The stored elastic deformation energy of the eyelid caused the hydrogel and lower eyelid to retract back towards the globe. This provided a realistic precompression of the hydrogel against the globe. An upward eye movement, representative of a quick 60° saccade[23] was simulated by rotating the globe around its center axis. Representative images of each step, and the applied rotation trace can be found in supplementary material Figure S1.

Contact between the eyelid and globe was defined as frictionless, and contact of the hydrogel with either side of the globe and eyelid was defined with coefficient of friction values (μ_{globe} or μ_{lid}). Values used for these contact interactions are described in Section "Geometry Comparison." Coefficient of friction values are considered to be constant throughout the duration of the simulation. Any changes in lubrication upon placement of the hydrogel in the eye are not anticipated in the very short amount of time represented in the simulation. Long-term changes in lubrication were not considered because the focus of this study was on the immediate response of the hydrogel in the eye. All simulations were performed using an explicit solver.

Simulation Study Design

Geometry Comparison

As the coefficients of friction between the chosen hydrogel film formulation (CMHA-S) and the sclera (μ_{globe}) and eyelid (μ_{lid}) are not known, all eight hydrogel geometries were tested in model iterations of

TABLE 1. Summary of material properties used in the human eye FEM.

Model component	Constitutive model	Model parameters	Poisson's ratio	Density (g/cm^3)	Reference
Hydrogel Film	Hyperelastic Marlow	$G_1 = 0.0334$	0.49	1	2, 5, 7, 13
	Viscoelastic Prony-series	$\tau_1 = 4.79$			
Eyelid	Linear-elastic	$E = 58.2$ MPa	0.49	1.05	1, 6, 11, 14
Globe	Discrete rigid body		–	–	–

differing μ_{lid}:μ_{globe} ratios. A low μ_{globe} value of 0.05 was chosen as this is a common coefficient of friction that is found in low-friction, high-water, hydrogel contact lenses,[19] and is assumed to be comparable to the coefficient of friction of the CMHA-S film. This low μ_{globe} was held constant for every simulation, and each geometry was tested at increasing μ_{lid} values that resulted in μ_{lid}:μ_{globe} ratios ranging from 1 to 3.5 (μ_{lid} = 0.05, 0.075, 0.1, 0.125, 0.15, and 0.175).

For each simulation, nodal displacements of the hydrogel films were extracted at the beginning of the rotation step, and at every 15 ms thereafter until the conclusion of the simulation. Nodal displacements were normalized so as to only include film displacement due to globe movement and not from placement of the films. Mean nodal displacements were calculated for every time point and compared across geometries.

Regression and correlation analyses were performed to evaluate the effect of geometry characteristics, contact area and friction ratio on hydrogel film displacement. Geometry characteristics included the thickness, length, width and volume of the film. Contact area evaluation included the total, lid-side and globe-side contact areas, and the ratio between lid-side and globe-side contact areas. The friction ratio was defined as the ratio of μ_{lid} to μ_{globe}. Main effects and correlations were significant at a p value less than 0.05. Correlation coefficients greater than 0.8 were considered strongly correlated, while coefficients less than 0.8 were considered weakly correlated. Interaction effects were not evaluated due to limited geometries and data.

Parametric Friction Study

To better understand the relationship between μ_{lid} and μ_{globe}, a parametric study was conducted to find the optimal relationship that completely immobilized the film in the lower eyelid. Geometry 5 was used for this study. Globe-side coefficient of friction (μ_{globe}) was increased from 0 to 2 at general increments of 0.02. At each value, lid-side coefficient of friction (μ_{lid}) was increased by increments of 0.01 until the film was immobilized. The film was considered successfully immobilized when the center node of the film displaced less than 0.05 mm during the rotation step.

RESULTS

Geometry Comparison

Eyelid retraction towards the globe resulted in a pocket formation around the hydrogel film, and the pocket shape was unique to each geometry. Cross-sectional views of the hydrogel film in the lower eyelid pocket can be seen in Fig. 4. Contact areas on either the lid or the globe side of the hydrogel ranged from 40 to 90 mm^2 (supplementary material Fig. S2). A minimal amount of compression occurred across the thickness of each geometry following the placement step of the hydrogel. The amount of compression was no more than 6% of its original thickness. No change in shape was seen during eye rotation.

Perfectly cylindrical geometries (i.e., Geometries 1 and 4) completely dislodged from the lower fornix at all iterations of μ_{lid}, and were therefore excluded from further analysis. Equal friction on either side of the hydrogel film ($\mu_{globe} = \mu_{lid} = 0.05$) resulted in complete dislodging of all geometries from the lower fornix (supplementary material Fig. S3). Increasing μ_{lid} to 0.075 ($\mu_{globe} = 0.05$) caused Geometries 2 and 8 to stay in the lower eyelid throughout the duration of globe movement, however all other geometries dislodged. It was not until μ_{lid} was at least two times that of μ_{globe} ($\mu_{lid} \geq 0.1$) that all geometries remained in the lower fornix (Fig. 5).

Generally, as μ_{lid} increased, average nodal displacement in all six geometries decreased. For all iterations of $\mu_{lid} \geq 0.1$, Geometry 7 displaced the least. Its displacement was at or below 0.05 mm, which was the threshold for immobilization defined in the friction optimization study in Section "Parametric Friction Study." Geometry 7 was also least affected by increasing μ_{lid} values, meaning that the decrease in displacement with increasing μ_{lid} was less than the other geometries. Geometry 2 was the next best performer, and also was not strongly affected by changing μ_{lid}. However, not all geometries were as impervious to the increasing ratio of μ_{lid}:μ_{globe}. Geometry 5 displaced the most at small values of μ_{lid}, but displacement was substantially reduced by 94% at higher μ_{lid} values. Differences in displacement between the geometries became smaller with increasing μ_{lid}, and all but one geometry (Geometry 3) displaced less than or equal to the immobilization threshold of 0.05 mm at $\mu_{lid} = 0.175$.

In the regression analysis, the ratio of friction on either side of the hydrogel film was the only factor that was significantly predictive of hydrogel film displacement. Thickness and volume of the hydrogel films were moderately correlated with displacement and had higher correlation coefficients ($0.60 < r < 0.75$) than the rest of the factors ($r < 0.50$). However, these correlations were found to be insignificant with p-values between 0.1 and 0.2. Examples of correlations can be seen for thickness, volume, total contact area, and lid-side to globe-side contact area for $\mu_{lid} = 0.175$ in Fig. 6.

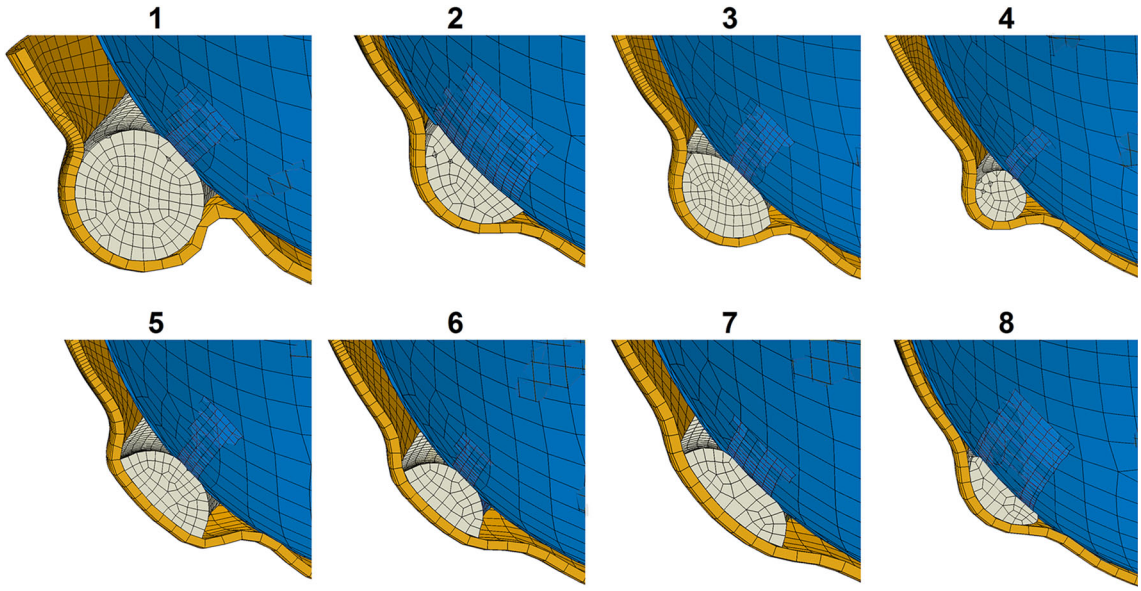

FIGURE 4. Cross-sectional images showing hydrogel film placed in lower fornix following eyelid retraction back towards the globe. Film geometry and the pocket that formed around the film were important in dictating film displacement.

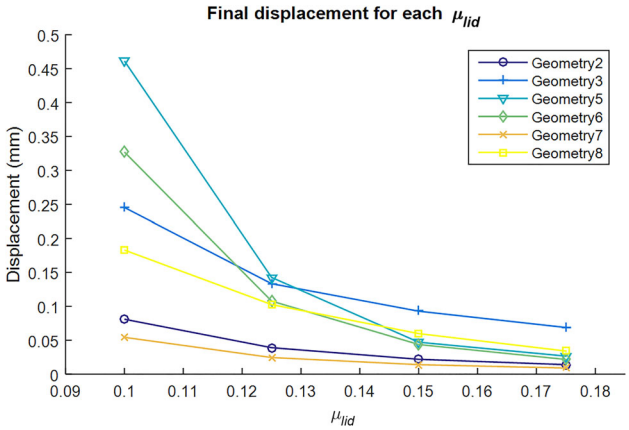

FIGURE 5. Mean nodal displacement found at the end of each simulation is shown for all hydrogel film geometries at increasing μ_{lid}. Globe-side friction is held constant throughout simulations ($\mu_{globe} = 0.05$). Only ratios that resulted in displacement < 0.5 mm are shown for clarity (μ_{lid}:μ_{globe} = 2, 2.5, 3 and 3.5). Changing μ_{lid} disproportionately affected the geometries' displacements, however as μ_{lid} increased, differences between the geometries' displacements decreased. Cylindrical Geometries (i.e., Geometries 1 and 4) dislodged from the inferior fornix at every value of μ_{lid}, and were excluded from analysis.

Friction Parametric Evaluation

The ratio of coefficients of friction between the hydrogel film and the eyelid/globe interfaces (μ_{lid}:μ_{globe}) required for immobilization in the lower eyelid (displacement < 0.05 mm) was found to be linear and described by the equation: $\mu_{lid} = 1.4 \times \mu_{globe} + 0.07$ (Fig. 7). Specifically, the coefficient of friction on the lid side of the film must be approximately 1.4 times larger than the globe side of the film to resist noticeable displacement during vertical globe movement. If the interaction between the hydrogel and the globe is frictionless, the ideal friction coefficient between the hydrogel and eyelid would need to be greater than 0.07.

DISCUSSION

The objectives of this study were to use FE analysis to determine potential geometrical designs of the hydrogel for improved retention, and to identify optimal surface friction ratios between the hydrogel and the globe or eyelid for immobilization in the inferior fornix. It was found that the hydrogel film's tendency to displace was influenced by both the geometrical design and the surface friction ratio, but friction was the only factor that was significantly predictive of the hydrogel film displacement. This may be due to the discrete evaluation of multiple geometries instead of a systematic evaluation of one geometry with varying length, width and thickness.

Differences between the cross-sectional shapes, lengths and orientations of each of the geometries affected the way the lower eyelid formed around the hydrogel upon placement, and is hypothesized to be a mechanism of action for resisting hydrogel film displacement during globe movement. Cylindrical geometries (i.e., Geometries 1 and 4) performed worse than all other geometries, and did not stay in the inferior fornix at any model iteration of μ_{lid}. These geometries physically rolled across the globe and out of

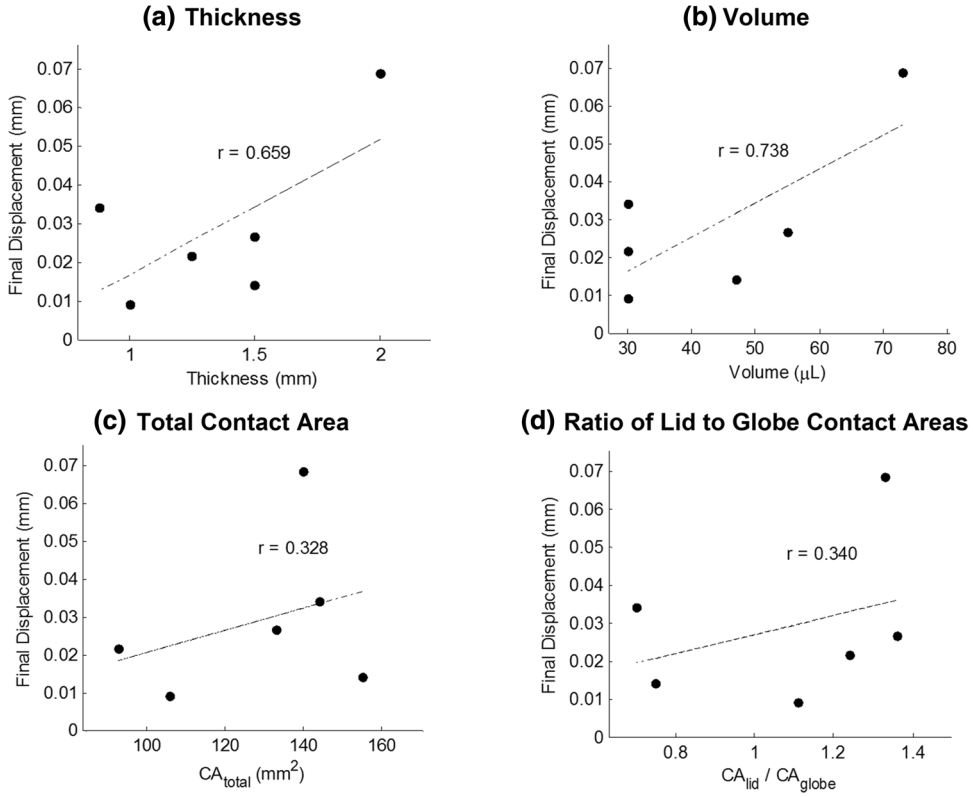

FIGURE 6. Correlation analyses between displacement and geometry factors of (a) cross-sectional thickness, (b) volume, (c) total contact area, and (d) ratio of contact area of the lid to contact area of the globe for μ_{lid} = 0.175. None of the factors were significantly correlated ($p < 0.05$) with displacement.

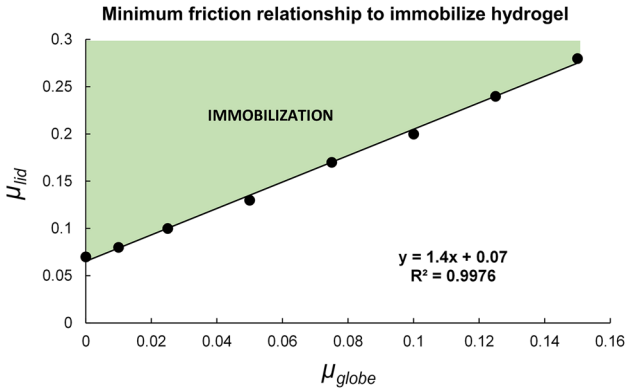

FIGURE 7. Relationship between friction of the hydrogel film with the lid (μ_{lid}) and globe (μ_{globe}) that is required to immobilize Geometry 5 in the inferior fornix of the eye during regular vertical eye movement.

the lower eyelid pocket. The flatter and less bulky geometries tended to perform better, with Geometries 7 and 2 displacing the least. However, an exception to this observation was found in Geometry 8. This geometry was the thinnest of the geometries (0.88 mm thick), and was notably the most discrete in the inferior fornix pocket. This geometry was also the longest geometry, which in addition to its thinness, caused its ends to easily flex upwards with globe rotation. While this geometry was mostly stationary in the pocket, the flexing mechanism contributed to the higher average nodal displacements that were yielded by this geometry. Geometry 3, which was more cylindrical in shape than the other geometries, was another of the worst-performing geometries of the study. This geometry yielded the greatest displacement of the retaining geometries at higher μ_{lid} values. This was not due to a rolling motion as seen in the perfect cylinders. Rather, it was much bulkier than the other geometries, and the eyelid was less able to resist movement caused by rotation.

Contact area of the hydrogel film's surfaces with the globe or eyelid was seen to have no effect on the displacement of the film. Coulomb friction is independent of surface area if small deformations are observed. All hydrogel deformations in these studies were $< 6\%$, which corresponds with our finding of no relationship of contact area to film displacement. Therefore, we believe the differences in displacement of each geometry are due to the pocket formed around the hydrogel when placed in the inferior fornix. Pockets that conformed to most of the geometry (Geometries 2, 7, and 8) were better retained than those that left large gaps around the geometry (Geometries 1, 3, 5, and 6).

Since overall changes in the cross-sectional shape and length affected the displacement of the hydrogel film, a more systematic design optimization of hydrogel size will be required to identify geometrical characteristics that improve retention. Dimensions, such as length, thickness, and width, can be parametrically evaluated in future studies on a single geometry to identify geometry modifications that are least disruptive to lower eyelid retention. This will be important for future design iterations that require volumetric changes to accommodate different drug loading volumes.

One of the most critical design aspects learned from the FE simulations was that while geometry was an important factor in mitigating hydrogel film displacement, controlling the friction will be the most effective mechanism of reducing displacement. As friction on the lid side of the hydrogel (μ_{lid}) increased, displacement of all retaining geometries decreased. Furthermore, as μ_{lid} increased, the difference in displacement between the geometries became smaller. At $\mu_{lid} = 0.175$, all geometries displaced less than 0.06 mm, with five out of six geometries displacing less than the threshold for immobilization (0.05 mm). These small differences in displacement at high μ_{lid} were considered to be negligible.

It is important to reiterate that hydrogel displacement was not influenced by just μ_{lid}, but rather by a relationship of μ_{lid} to μ_{globe}. In order to mitigate displacement, the hydrogel needs to stick more to the eyelid than it does to the globe; that is, μ_{lid} must be greater than μ_{globe}, so that it can slip against the globe surface during eye rotation. Specifically, the FE model determined that a relationship of $\mu_{lid} \geq 1.4 \times \mu_{globe} + 0.07$ was optimal for completely immobilizing Geometry 5 in the lower eyelid. However, this relationship likely does not apply for all geometries, because each geometry was uniquely affected by changing the μ_{lid} to μ_{globe} ratio. Geometry 5 was most strongly influenced by this ratio, and reduced displacement by 0.43 mm over μ_{lid} of 0.1 through 0.175. Geometries 7 and 2 were least affected by an increased μ_{lid}:μ_{globe} ratio with final displacements reduced by 0.05 and 0.07 mm, respectively. Therefore, the linear relationship identified for Geometry 5 presumably defines a worst-case scenario. Relationships for the other geometries will likely require smaller friction ratios. Future studies are planned to find an optimal relationship of μ_{lid} to μ_{globe} that is independent of geometry.

Another important finding from the model was that equal friction on either side of the hydrogel caused the hydrogels to immediately dislodge from the inferior fornix. This finding was confirmed by animal studies investigating the retention and tolerability of some of the designed geometries in the inferior fornix of rabbits (unpublished data). The geometries tested *in vivo* were not designed to have different coefficients of friction on either side of the hydrogel, and they were not retained reliably. Many geometries dislodged from the inferior fornix within hours. To generate different frictional properties on each side of the hydrogel, modifications to the hydrogel surface that increase roughness or adhesion will need to be made on the side that comes into contact with the lower eyelid. Examples of methods to achieve this include texturing the surface with micropatterns, or integrating an adhesive layer into the polymer.

During development of the FE model, inclusion of the complex inferior fornix anatomy was considered. Due to the challenging nature of precisely replicating the anatomy, it was decided to simplify the structure but maintain the contour to the surface of the globe and the pocket-like formation of the inferior fornix. One limitation of this simplification is that this pocket representation was symmetrical and did not account for inferior fornix asymmetry or non-uniform interactions with the globe or CMHA-S film. Therefore, this simplification limited the ability of the study to evaluate the geometry when placed in different locations of the inferior fornix pocket. It is possible the film geometry and its specific placement *in vivo* may have a greater effect on retention than found in this study.

This FE representation models the hydrogel film in a healthy eye. Since these films will presumably be used to treat an injured or diseased eye, it is important to consider how the films will behave under altered and pathological circumstances. An injured eye will be highly inflamed and swollen, and may increase the pressures enacting on the film from the eye and eyelid. The conjunctiva may have excessive inflammation, swelling, and an altered mucosal surface, thus rendering it more mucoadhesive. In which case, the film is hypothesized to be held more tightly in place than in the healthy model, and is more likely to resist movement and dislodging. However, it is also thought that the inflammatory response in an injured or diseased eye will contribute to an increase in degradation rate of the hydrogel causing it to lose mass and overall shape more quickly. It is unclear how the polymer's degradation over time changes its shape and retention in the eye, therefore further investigation will be needed to characterize the longer-term degradation of the polymer.

One final limitation of the FE model is the lack of available validation data. It will be challenging to develop a test setup to monitor displacement of the CMHA-S film in an *in vivo* model to validate FE model predictions. However, the results presented in this study are purely comparative of geometry and friction interactions, and not predictive of stresses or

strains seen in the eye. Therefore, conclusions made herein of the effects of geometry and friction are still valid without supporting validation data.

CONCLUSION

Retention of the hydrogel film in the inferior fornix was dependent on hydrogel geometry and the ratio of friction on the hydrogel to the eyelid and globe. The effectiveness of reducing displacement by these factors was interactive. At low μ_{lid} to μ_{globe} ratios, geometry played a role in a films tendency to displace with the flatter and less bulky geometries displacing less than the geometries that were cylindrical. However, at high μ_{lid} to μ_{globe} ratios, the effect of displacement due to geometrical differences was minimal. Despite these observations, only the ratio of μ_{lid} to μ_{globe} was found to significantly influence displacement. Therefore, careful control of friction will be the focus of future studies. A systematic evaluation of the effects of length, width and thickness on film slip is still necessary to guide geometry modifications for drug volume requirements.

ELECTRONIC SUPPLEMENTARY MATERIAL

The online version of this article (https://doi.org/10.1007/s10439-017-1962-x) contains supplementary material, which is available to authorized users.

ACKNOWLEDGMENTS

This material is based upon work supported by the National Science Foundation under Award Number IIP-1430921, and the Department of Defense under Award Number W81XWH-14-C-0025. Any opinions, findings, and conclusions or recommendations expressed in this abstract are those of the authors and do not necessarily reflect the views of the National Science Foundation or the Department of Defense.

DISCLOSURES

Dr. Barbara Wirostko co-founded Jade Therapeutics Inc. and holds intellectual property relating to the use of the polymer. Additionally, she discloses a financial relationship with EyeGate Pharmaceuticals Inc. in the form of employment and stock ownership. The remaining authors have no conflicts of interest to disclose.

REFERENCES

[1]Annaidh, A. N., K. Bruyre, M. Destrade, M. D. Gilchrist, and M. Ottnio. Characterization of the anisotropic mechanical properties of excised human skin. *J. Mech. Behav. Biomed. Mater.* 5:139–148, 2012.

[2]Appel, E. A., X. J. Loh, S. T. Jones, F. Biedermann, C. A. Dreiss, and O. A. Scherman. Ultrahigh-water-content supramolecular hydrogels exhibiting multistimuli responsiveness. *J. Am. Chem. Soc.* 134:11767–11773, 2012.

[3]Blum, M. M., and T. C. Ovaert. Low friction hydrogel for articular cartilage repair: evaluation of mechanical and tribological properties in comparison with natural cartilage tissue. *Mater. Sci. Eng. C* 33(7):4377–4383, 2013.

[4]Chang, D. F. Chapter 2 Ophthalmologic Examination. In: Asbury's General Ophthalmology18th, edited by P. Riordan-Eva, and E. P. CunninghamVaughan. New York: The McGraw-Hill Companies, 2011.

[5]Coats, B., M. M. Drysdale, H.-K. Lee, and B. M. Wirostko. Mechanical properties of four carboxymethylated hyaluronic acid hydrogel polymer formulations. *Invest. Ophthalmol. Vis. Sci.* 56:4167, 2015.

[6]Gallagher, A. J., A. N Annaidh, K. Bruyre, and E. Al. Dynamic tensile properties of human skin. In: Proceedings of the International Research Council on the Biomechanics of Injury, 2012.

[7]Gayet, J. C., and G. Fortier. High water content BSA-PEG hydrogel for controlled release device: evaluation of the drug release properties. *J. Control. Release* 38:177–184, 1996.

[8]Gum, G. G., B. M. Wirostko, M. Rafii, V. Naageshwaran, M. Lyulkin, R. Merideth, and B. Mann. Safety assessment of a novel, cross-linked, bio-absorbable carboxymethyl hyaluronic acid (CMHA) polymer in a rabbit ocular surface model. *Invest. Ophthalmol. Vis. Sci.* 56(7):1297, 2015.

[9]Hennessy, A. L., J. Katz, D. Covert, C. A. Kelly, E. P. Suan, M. A. Speicher, N. J. Sund, and A. L. Robin. A video study of drop instillation in both glaucoma and retina patients with visual impairment. *Am. J. Ophthalmol.* 152:982–988, 2011.

[10]Hennessy, A. L., J. Katz, D. Covert, C. Protzko, and A. L. Robin. Videotaped evaluation of eyedrop instillation in glaucoma patients with visual impairment or moderate to severe visual field loss. *Ophthalmology* 117:2345–2352, 2010.

[11]Liang, X., and S. A. Boppart. Biomechanical properties of *in vivo* human skin from dynamic optical coherence elastography. *IEEE Trans. Biomed. Eng.* 57(4):953–959, 2010.

[12]Liu, X., H. Nanao, T. Li, and S. Mori. A study on the friction properties of PAAc hydrogel under low loads in air and water. *Wear* 257(7–8):665–670, 2004.

[13]Marlow, R. S. A general first-invariant hyperelastic constitutive model. In: Constitutive Models for Rubber, pp. 157–160, 2003.

[14]Morales, M. F., E. N. Rathbuk, R. E. Smith, and N. Pace. Studies on body composition. 2. Theoretical considerations regarding the major body tissue components, with suggestions for application to man. *J. Biol. Chem.* 158:677–684, 1945.

[15]Moss, S., R. Klein, and B. Klein. Prevalence of and risk factors for dry eye syndrome. *Arch. Ophthalmol.* 118:1264–1268, 2000.

[16]Quigley, H. A. Glaucoma. *Lancet* 377(9774):1367–1377, 2011.

[17]Quigley, H. A., and A. T. Broman. The number of people with glaucoma worldwide in 2010 and 2020. *Br. J. Ophthalmol*. 90:262–267, 2006.
[18]Rafii, M., B. Wirostko, G. G. Gum, K. Godfrey, and H.-K. Lee. Safety, tolerability, of ocular sustained-release (SR) moxifloxacin (MX) hydrogel films in New Zealand White (NZW) rabbits for corneal ulcers. *Invest. Ophthalmol. Vis. Sci*. 55(13):4704, 2014.
[19]Roba, M., E. G. Duncan, G. A. Hill, N. D. Spencer, and S. G. P. Tosatti. Friction measurements on contact lenses in their operating environment. *Tribol. Lett*. 44:387–397, 2011.
[20]Robin, A. L., G. D. Novack, D. W. Covert, R. S. Crockett, and T. S. Marcic. Adherence in glaucoma: objective measurements of once-daily and adjunctive medication use. *Am. J. Ophthalmol*. 144:533–540, 2007.
[21]Short, B. G. Safety evaluation of ocular drug delivery formulations: techniques and practical considerations. *Toxicol. Pathol*. 36:49–62, 2008.
[22]Toole, B. P. ''Hyaluronan in Morphogenesis'', in Seminars in Cell & Developmental Biology. Amsterdam: Elsevier, pp. 79–87, 2001.
[23]Von Noorden, G. K., and E. C. Campos. Physiology of the ocular movements. *Binocul. Vis. Ocul. Motil*. 5:53–80, 2002.
[24]Williams, D. L., and B. K. Mann. A crosslinked HA-based hydrogel ameliorates dry eye symptoms in dogs. *Int. J. Biomat*. 2013. https://doi.org/10.1155/2013/460437.
[25]Yang, G., L. Espandar, N. Mamalis, and G. D. Prestwich. A cross-linked hyaluronan gel accelerates healing of corneal epithelial abrasion and alkali burn injuries in rabbits. *Vet. Ophthalmol*. 13(3):144–150, 2010.
[26]Zarembinski, T. I., N. J. Doty, I. E. Erickson, R. Srinivas, B. M. Wirostko, and W. P. Tew. Thiolated hyaluronan-based hydrogels crosslinked using oxidized glutathione: an injectable matrix designed for ophthalmic applications. *Acta Biomater*. 10(1):94–103, 2014.